

Is the combination of MR and CT findings useful in determining the tumor grade of pancreatic neuroendocrine tumors?

Fumihito Toshima¹ · Dai Inoue¹ · Takahiro Komori¹ · Kotaro Yoshida¹ · Norihide Yoneda¹ · Tetsuya Minami¹ · Osamu Matsui¹ · Hiroko Ikeda² · Toshifumi Gabata¹

Received: 24 October 2016 / Accepted: 19 February 2017 / Published online: 3 March 2017
© Japan Radiological Society 2017

Abstract

Purpose To retrospectively elucidate the findings useful in determining the tumor grade of pancreatic neuroendocrine tumors (PNETs) by combined assessment of magnetic resonance (MR) and dynamic computed tomography (CT) images.

Materials and methods Eighty-nine patients with PNETs (96 lesions) were included, and classified as G1, 59; G2, 29; and G3, 8 lesions. Image analysis included lesion diameter, shape, enhancement pattern on arterial phase (AP) and delayed phase CT images, calcification, cystic portion, main pancreatic duct dilatation, signal-intensity on T1-, T2-weighted MR images, and appearance of apparent diffusion coefficient (ADC).

Results Significant differences among G1, G2, and G3 groups were noted in tumor maximal diameter ($p < 0.0001$), shape ($p < 0.0001$), enhancement pattern on AP image ($p < 0.0001$), cystic portion ($p = 0.012$), and ADC finding. In multivariate analysis, ADC finding was the independent factor ($p = 0.002$). The combination findings of

low ADC ratio (ADC value of the lesion/ADC value of the parenchyma < 0.94), not homogeneous hyper-attenuation, lobulated shape, and hyper-intensity on T2-weighted image were suggestive of G2 or G3 with a probability of 100%. Conversely, all lesions with high ADC ratio and small size (≤ 25 mm) belonged to the G1 group.

Conclusion Combined assessment of MR and CT findings could improve the prediction of tumor grading in PNETs.

Keywords Pancreatic neuroendocrine tumors · Neuroendocrine tumors G1 · Neuroendocrine tumors G2 · Neuroendocrine carcinoma · Magnetic resonance imaging (MRI) · Computed tomography (CT)

Introduction

Pancreatic neuroendocrine tumors (PNETs) are rare pancreatic tumors with a prevalence of approximately one in 100,000 persons, accounting for 1–2% of all pancreatic neoplasms [1]. Recently, with improvements in imaging

This study was approved by our institutional review board.

✉ Fumihito Toshima
fumihitotoshima@gmail.com

Dai Inoue
Inoue.Dai@mayo.edu

Takahiro Komori
kmrkhr0627@gmail.com

Kotaro Yoshida
kotaroy@med.kanazawa-u.ac.jp

Norihide Yoneda
noritin@f7.dion.ne.jp

Tetsuya Minami
tminami@staff.kanazawa-u.ac.jp

Osamu Matsui
matsuo@med.kanazawa-u.ac.jp

Hiroko Ikeda
h-ikeda@med.kanazawa-u.ac.jp

Toshifumi Gabata
gabata@med.kanazawa-u.ac.jp

¹ Department of Radiology, Kanazawa University Graduate School of Medical Science, 13-1 Takara-machi, Kanazawa, Ishikawa 920-8641, Japan

² Department of Pathology, Kanazawa University Graduate School of Medical Science, 13-1 Takara-machi, Kanazawa, Ishikawa 920-8641, Japan

techniques and the spread of endoscopic ultrasonography-guided fine needle aspiration (EUS-FNA), the detectability of small lesions has improved [2].

All PNETs are supposed to have potential malignancy, but have a wide spectrum of aggressiveness and growth pattern [2]. In 2010, the World Health Organization (WHO) classification that differentiated the tumor grade of malignancy was modified, and is now widely used in clinical practice [3]. This classification differentiated PNETs into neuroendocrine tumors G1, G2 and neuroendocrine carcinoma (G3) based on the mitotic count and Ki-67 labeling index [3–6]. This grading system has emerged as the most potent predictive factor in many studies [7, 8].

Previous studies have suggested the possibility of imaging examinations as a useful modality to determine the tumor grade [9–19]. However, most of them used a single modality, or focused on only a small number of cases, and thus whether widely used imaging examinations can determine the tumor grade is still controversial. The purpose of this study was to retrospectively elucidate the findings useful in determining the tumor grade of PNETs by combined assessment of magnetic resonance (MR) and dynamic computed tomography (CT) images.

Materials and methods

Case selection

This study was approved by our institutional review board, with informed consent waived because of its retrospective nature. It consisted of 101 consecutive patients (55 men and 46 women; mean age, 60 ± 13 years; range 12–87 years) with pathologically proven PNETs with use of pancreatic specimens (surgical resection, $n = 92$; and EUS-FNA, $n = 9$, respectively). This study did not contain any patients in whom the pathological diagnosis and tumor grading were performed using metastatic specimens, because of the possibility of a mismatch in the grading between the primary pancreatic lesion and metastasis. All patients were selected from the pathology files of our hospitals and eight related institutions from the period between January 2006 and June 2016. Imaging data were available for all patients. The mean period between final imaging (CT or MR) examination and pathological diagnosis was 36 ± 32 days (range 0–150 days). Of 101 patients, eight were excluded because of insufficient imaging examinations for evaluation of the detailed radiological findings (small [< 5 mm] lesion, $n = 7$; and only plain CT image, $n = 1$), and four were excluded because they contained other tumor components. Eventually, 89 patients (96 lesions) were included in this study.

All PNETs were diagnosed on the basis of the histologic findings of hematoxylin-eosin staining, and immunohistochemical expression of chromogranin A and synaptophysin. Moreover, tumor grading was done by counting the number of mitoses per 10 high-power fields, and evaluating the Ki-67 proliferation index. Evaluation of the Ki-67 index was performed using immunohistochemistry with MIB-1 antibody at the level of the maximal diameter of the tumor. All specimens were collected to our institution and re-evaluated by a single pancreatic pathologist with 14 years' experience. In the histopathologic analysis of 96 PNETs, 59 lesions (61.5%) were classified as G1; 29 (30.2%), as G2; and 8 (8.3%), as G3.

Imaging examinations

CT imaging

Computed tomography images were available for all 89 patients (96 lesions). Multi-detector row CT examinations were performed with a tube voltage of 120–135 kVp, and an automatic exposure control system. Because of the multi-institutional, retrospective nature of the study, several CT scanners were used.

All 89 patients underwent non-enhanced and contrast enhanced multiphase (at least two phases, arterial phase [AP], and delayed phase [DP]) dynamic CT. AP and DP images were obtained at 30–45 s, and at more than 120-s delays, after starting the rapid intravenous injection of non-ionic contrast medium using a power injector. Early arterial phase (20- to 30-s delay), and portal venous phase (60- to 75-s delay) images were available for 53, and 55 patients, respectively. However, these phase images were not assessed in this study. Because of the multi-institutional nature of this study, several contrast media with different iodine concentrations (300–370 mg/ml) were used.

MR imaging

Magnetic resonance images were available for 79 (88.8%) of 89 patients (86 lesions). Several 1.5 or 3T MR scanners were used. All protocols included transverse T1-weighted (2 or 3 dimension gradient-recalled-echo, dual gradient-echo, and/or fast-spin-echo) and T2-weighted (fast-spin-echo, single-shot fast-spin-echo, and/or fast-recovery fast-spin-echo) images. Echo-planar diffusion-weighted (DW) images using two b values (0–800 s/mm², 48 patients; 0–1000, 4 patients) were available for 52 patients (56 lesions). Because of the multi-institutional retrospective nature of this study, the scanning protocols were not consistent.

Of CT and MR examinations, the initial examination was CT in 63 patients, and MR in 16 patients. The

mean period between CT and MR examinations was 23 ± 24 days (range 0–97 days).

Image analysis

All images were independently reviewed by two radiologists with 10 and 15 years' experience in pancreatic radiology, who were blinded to final tumor grade. If the decisions of the two radiologists were different in subjective parameters, consensus was finally reached through discussion after a reviewing session, and simple and quadratic weighted kappa values were calculated to evaluate the inter-reader reproducibility. CT and MR images were analyzed for the following parameters for each lesion: lesion maximal diameter, lesion shape (round, lobulated, or irregular), enhancement pattern on AP CT image (homogeneous hyper-, homogeneous iso-, homogeneous hypo-attenuation, or heterogeneous attenuation), presence or absence of gradual enhancement on DP CT image, presence or absence of calcification, cystic portion, hemorrhage, and main pancreatic duct (MPD) dilatation, signal-intensity on T1-weighted, and T2-weighted MR image (hypo-, iso-, or hyper-intensity), appearance on apparent diffusion coefficient (ADC) map, and ADC ratio.

Lesion diameter and shape were evaluated using multi-planner reconstruction CT images in all cases. Measuring lesion diameter was determined by consensus of two radiologists. Enhancement pattern on AP image, and signal-intensity on MR image of solid portions were visually determined by comparison with the surrounding pancreatic parenchyma.

The value of AP and DP images was individually measured by placing a region of interest (ROI) on the solid portion of the lesion. The ROI was drawn to be as large as possible by using a free curve. The ROI location was also determined by consensus of two radiologists. The average size of the ROI was 502 ± 995 mm² (range 15–4682 mm²). Gradual enhancement on CT image was determined to be present when the average attenuation value of the lesion increased between AP and DP images. In evaluation for diffusion-weighted images, the ADC value itself was not analyzed because of the inconsistency of the MR scanners; instead we evaluated by using two methods, visual estimation (reduction or no reduction in ADC compared with the surrounding pancreatic parenchyma), and ADC ratio (ADC value of the lesion/ADC value of the pancreatic parenchyma). The ADC value of the lesion was measured in the same way as the evaluation of gradual enhancement. The average size of ROI was 376 ± 840 mm² (range 17–4807 mm²). The ADC value of the parenchyma was measured by placing ROI (size, 100 mm²; shape, round or oval) on the pancreatic parenchyma of the proximal side of the lesion.

The cystic portion was defined as non-enhanced areas and/or hyper-intensity similar to the cerebrospinal fluid on T2-weighted images. Hemorrhage was defined as hyperdense areas on non-contrast-enhanced CT images and/or hyper-intensity on T1-weighted images. These imaging findings were compared among G1, G2, and G3 groups.

Statistical analysis

Statistical significance was evaluated using GraphPad Prism 6 (GraphPad Software, San Diego, Ca), R version 3.2.2 (R Foundation for Statistical Computing, Vienna, Austria), and SPSS 23.0 (SPSS Inc, Tokyo, Japan). Fisher's exact test or Kruskal–Wallis test with multiple comparison test was used to compare the imaging findings among all groups. Additionally, multinomial logistic regression between the tumor grade (G1, G2, or G3) and the imaging findings, which showed significant differences in univariate analysis, was performed to find the independent factors. Sensitivity, specificity, positive predictive value (PPV), negative predictive value (NPV) and odds ratio in the prediction of the G1 group for imaging findings, alone and in association with others, were calculated. The cutoff values with the best sensitivity and specificity in lesion diameter and ADC ratio using ROC curves were calculated. A *p* value less than 0.05 was considered to indicate a statistically significant difference. Regarding inter-reader reproducibility, simple kappa values of lesion shape, enhancement pattern on AP CT images, presence or absence of calcification, cystic portion, hemorrhage, MPD dilatation, and appearance on ADC map, and weighted kappa values of signal-intensity on T1-weighted, and T2-weighted images were calculated. A kappa value less than 0.20 was interpreted as poor agreement, in the range of 0.21–0.40 as fair agreement, 0.41–0.60 as moderate agreement, 0.61–0.80 as good agreement, and more than 0.81 as excellent agreement.

Results

Imaging findings of all lesions

The average maximal diameter of the lesions was 28 ± 25 mm (range 6–142 mm). Thirty-two lesions (33.3%) were located in the head, 32 (33.3%) in the body, and 32 (33.3%) in the tail. The lesions appeared as round masses in 78 (81.3%), and as lobulated ones in 18 (18.7%). Lesions with irregular shape were not found.

Solid portions of all 96 lesions were nearly iso-attenuating compared to the surrounding pancreatic parenchyma on non-contrast-enhanced CT images. On AP images, 51 lesions (53.1%) were described as homogeneous

hyper-attenuation. Homogeneous hypo-attenuation, and heterogeneous attenuation were shown in 14 lesions (14.6%), and 17 (17.7%), respectively. The remaining 14 lesions (14.6%) demonstrated homogeneous iso-attenuation, and were difficult to detect on AP images. On DP images, seven lesions (7.3%) showed gradual enhancement.

Calcifications, cystic portions, and MPD dilatations were found in 14 lesions (14.6%), 32 (33.3%), and 18 (18.7%), respectively, but hemorrhagic change was not found in any lesions.

All 86 lesions were hypo- ($n = 66$) or iso-intense ($n = 20$) on T1-weighted images, and 83 lesions (96.5%) were hyper- ($n = 47$) or iso-intense ($n = 36$) on T2-weighted images. Of 56 PNETs, ADC was visually reduced in 28 lesions (50.0%), compared with the surrounding pancreatic parenchyma on the ADC map, with others demonstrating iso- to hyper-intense.

Regarding inter-reader reproducibility of visually evaluated imaging parameters, kappa values of lesion shape, enhancement pattern on AP CT image, presence or absence of calcification, cystic portion, hemorrhage, MPD dilatation, signal-intensity on T1-weighted, and T2-weighted images, and appearance on ADC map were 0.87, 0.98, 1.0, 0.95, 1.0, 1.0, 0.95, 0.99, and 0.89, respectively.

Comparison among G1, G2 and G3 groups

Comparisons among G1, G2, and G3 groups for each of the imaging findings are summarized in Table 1. Significant differences among G1, G2, and G3 groups were noted in tumor maximal diameter, shape, enhancement pattern on AP CT image, cystic portion, and ADC finding.

Based on the results of statistical analysis with multiple comparison test, the maximal diameter of the lesion was significantly smaller in the G1 group than G2 or G3 group lesions (average maximal diameter, 18 versus 40, 56 mm, respectively; G1 versus G2, $p = 0.0004$; G1 versus G3, $p = 0.0005$) (Figs. 1, 2, 3). Moreover, the proportion of round lesions was significantly higher in the G1 group than in the G2 or G3 groups (G1 versus G2, $p = 0.0251$; G1 versus G3, $p = 0.0002$) (Figs. 1, 2, 3). The homogeneous hyper-attenuating lesions on AP CT images were most frequently seen in the G1 group as compared to the other groups (G1, 74.6; G2, 24.1; and G3, 0%, respectively). In contrast, the rate of homogeneous hypo-attenuating and heterogeneous attenuating lesions was higher in the G2 or G3 groups than in the G1 group (G2, 20.7 and 31.0; G3, 50.0 and 37.5; versus G1, 6.8 and 8.4%, respectively) (Figs. 1, 2, 3, 4). On DP images, gradual enhancement tended to be less frequently seen in the G1 group than the G2 or G3 groups, but without significant differences between any of the groups.

The frequency of a cystic portion was significantly higher in the G2 group than the G1 group (G1, 23.7%; G2, 55.2%; $p = 0.0137$). On the other hand, the rate of calcification and MPD dilatation also tended to be higher in the G2 group than the G1 group, but these differences were not significant between any of the groups.

On MRI, three lesions showed hypo-intensity on T2-weighted MR images. Of three, two lesions were pathologically diagnosed as G2, and one as G1. In visual assessment, reductions in ADC were less frequently seen in the G1 group than the G2 or G3 groups (G1, 29.4; G2, 76.5; and G3, 100%, respectively; G1 versus G2, $p = 0.0074$; G1 versus G3, $p = 0.0078$) on ADC maps (Figs. 1, 2, 3, 4, 5). The ADC ratio was significantly higher in the G1 group than the G2 or G3 groups (average ratio, 1.01 versus 0.78, 0.69, respectively; G1 versus G2, $p = 0.0008$; G1 versus G3, $p = 0.0067$).

Compared to the G2 group, the proportion of lobulated lesions was significantly higher in the G3 group ($p = 0.0345$). G3 lesions also demonstrated larger size, homogeneous hypo-enhancement or heterogeneous enhancement on AP image, delayed enhancement on DP image, hypo-intensity on ADC map, and lower ADC ratio, but none of these differences was significant.

Based on the results of multivariate analysis by multinomial logistic regression between the tumor grade and imaging findings (lesion maximal diameter, shape, cystic portion, enhancement pattern on AP CT image, and appearance on ADC map) in 56 lesions, in which all imaging parameters were evaluated, showed that appearance on ADC map was the only independent factor ($p = 0.002$).

Of 87 resected lesions (remaining 9 lesions diagnosed by EUS-FNA were excluded), significant differences among G1, G2, and G3 groups were also noted in tumor maximal diameter, shape, enhancement pattern on AP CT image, cystic portion, visual ADC estimation, and ADC ratio ($p = 0.0001$, $p = 0.0007$, $p < 0.0001$, $p = 0.0223$, $p = 0.0031$, and $p = 0.0004$, respectively).

Combined analysis of imaging findings

Sensitivity, specificity, PPV, NPV and odds ratio in the prediction of G1 group for each imaging finding are summarized in Table 2. PPVs and NPVs with small size (25 mm or smaller), round shape, homogeneous hyper-attenuation on AP image, absence of gradual enhancement on DP image, absence of calcification, absence of cystic portion, absence of MPD dilatation, iso-intensity on T1-weighted image, absence of hypo-intensity on T2-weighted image, no reduction in ADC compared with the pancreatic parenchyma (visual assessment), and high ADC ratio (0.94 or higher) were 77.3, 70.5, 86.3, 61.8, 63.4, 70.3, 64.1, 70.0, 62.7, 85.7, 92.3, and 73.3, 77.8, 66.7, 42.9, 50.0, 56.3, 50.0,

Table 1 Comparison among G1, G2, and G3 groups for each of imaging finding

	G1 group	G2 group	G3 group	<i>p</i> value
Lesion maximum diameter (mm)	18	40	56 ^a	<0.0001
Lesion shape				<0.0001
Round	55 (93.2%)	21 (72.4%)	2 (25.0%)	
Lobulated	4 (6.8%)	8 (27.6%)	6 (75.0%)	
Enhancement pattern on AP image				<0.0001
Homogeneous hyper-attenuation	44 (74.6%)	7 (24.1%)	0 (0%)	
Homogeneous iso-attenuation	6 (10.2%)	7 (24.1%)	1 (12.5%)	
Homogeneous hypo-attenuation	4 (6.8%)	6 (20.7%)	4 (50.0%)	
Heterogeneous attenuation	5 (8.4%)	9 (31.0%)	3 (37.5%)	
Gradual enhancement on DP image				NS
(+)	4 (6.8%)	2 (6.9%)	1 (12.5%)	
(−)	55 (93.2%)	27 (93.1%)	7 (87.5%)	
Calcification				NS
(+)	7 (11.9%)	5 (17.2%)	2 (25.0%)	
(−)	52 (88.1%)	24 (82.8%)	6 (75.0%)	
Cystic portion				0.012
(+)	14 (23.7%)	16 (55.2%)	2 (25.0%)	
(−)	45 (76.3%)	13 (44.8%)	6 (75.0%)	
MPD dilatation				NS
(+)	9 (15.2%)	7 (24.1%)	2 (25.0%)	
(−)	50 (84.8%)	22 (75.9%)	6 (75.0%)	
T1-weighted image				NS
Iso-intensity	14 (26.4%)	6 (23.1%)	0 (0%)	
Hypo-intensity	39 (73.6%)	20 (76.9%)	7 (100%)	
T2-weighted image				NS
Hyper-intensity	28 (52.8%)	13 (50.0%)	6 (85.7%)	
Iso-intensity	24 (45.3%)	11 (42.3%)	1 (14.3%)	
Hypo-intensity	1 (1.9%)	2 (7.7%)	0 (0%)	
Appearance on ADC map				0.0002
Reduction in ADC	10 (29.4%)	13 (76.5%)	5 (100%)	
No reduction in ADC	24 (70.6%)	4 (23.5%)	0 (0%)	
ADC ratio	1.01	0.78	0.69 ^b	<0.0001

Data are number of lesions, with percentages in parentheses

Statistical evaluation was performed among all groups by using Fisher's or Kruskal–Wallis test

AP arterial phase, DP delayed phase, MPD main pancreatic duct, ADC apparent diffusion coefficient

^a Data are mean values. Total numbers of lesions in G1, G2, and G3 groups were 59, 29, and 8 lesions, respectively

^b Data are mean values. Total numbers of lesions in G1, G2, and G3 groups were 34, 17, and 5 lesions, respectively

40.9, 66.7, 64.3, 66.7, respectively. PPV showed 89.1% (41 of 46 lesions) by applying the combination pertaining to three CT images [small size (25 mm or smaller), round shape, and homogeneous hyper-attenuation on AP image]. Conversely, the lesions with the opposite imaging findings (large size, lobulated shape, and no early enhancement pattern) belonged to G2 or G3 groups with a probability of 87.5 (14 of 16 lesions).

A grading flowchart based on the combination of MR and CT findings is shown in Fig. 6. This flowchart targeted

56 lesions in which all of the imaging parameters were analyzed. First, if the answers were 'Yes' to two questions pertaining to the MR and CT images, low ADC ratio ($0.94 >$), and not homogeneous hyper-attenuation on AP image, 17 of 22 lesions belonged to G2 or G3 groups (G2, $n = 12$; G3, $n = 5$). Of these, 12 lesions were small sized (25 mm or smaller), and 8 of 12 lesions belonged to G2 or G3 groups (G2, $n = 6$; G3, $n = 2$) (Fig. 4). Second, of 22 lesions ('Yes' group for first question), if the answers were 'Yes' to two questions, lobulated shape, and hyper-intensity

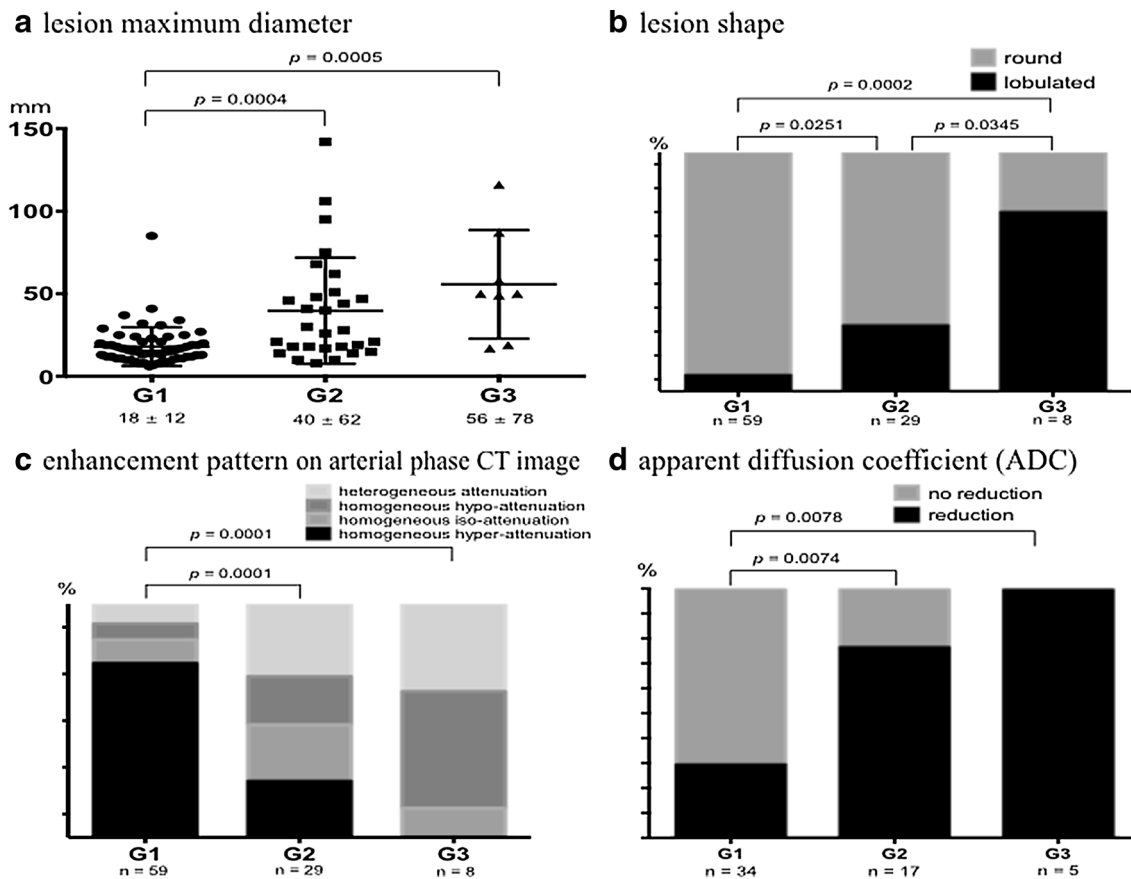


Fig. 1 Graphs show the comparison among G1, G2, and G3 groups. **a** Statistical significance in lesion maximal diameter is analyzed by using Kruskal–Wallis test with multiple comparison test. Mean value \pm standard deviation is given under the graph. **b–d** Significances in lesion shape, enhancement pattern on arterial phase (AP)

CT image, and appearance on apparent diffusion coefficient (ADC) map are analyzed by using Fisher’s exact test with multiple comparison test. **c, d** Visual assessments, by comparison with the surrounding pancreatic parenchyma, are performed

on T2-weighted image, the rate of G2 or G3 was 100% (G2, $n = 2$; G3, $n = 3$) (Fig. 3). Third, of 34 lesions (‘No’ group for first question), if the answers were ‘Yes’ (high ADC ratio [0.94 or higher], and small size [25 mm or smaller]), the rate of G1 lesions was 100% (20 of 20 lesions) (Fig. 2).

Discussion

Our results showed several imaging findings of PNETs, of which the following: smaller tumor size (≤ 25 mm), round shape, homogeneous hyper-attenuation on AP CT image, and no reduction in ADC compared with the pancreatic parenchyma by visual assessment (or high ADC ratio [0.94 \leq]) were predictive of G1, whereas larger tumor size, lobulated shape, homogeneous hypo-attenuation or heterogeneous attenuation, and reduction in ADC (or low ADC ratio) were suggestive of G2 or G3.

So far, several reports, including some of small numbers of cases, have focused on the imaging features useful in predicting the malignancy of PNETs. Similar to the results of this study, several CT findings such as tumor size, shape and vascularity of the tumor correlated with the tumor grade in recent studies [9–14]. Regarding vascularity, we assessed not only the AP image but also gradual enhancement on the DP image; however, no significant difference was detected. Degeneration (calcification or cystic portion), and MPD dilatation have been reported as predictive factors in some of the previous studies [13, 14]. This study also showed that the frequency of cystic degeneration, perhaps due to necrosis, was significantly higher in the G2 group than in the G1 group. Although the rate of calcification and MPD dilatation tended to be higher in the G2 group than in the G1 group, neither showed significant difference. We did not evaluate invasion of large vessels and adjacent organs, or the presence/absence of metastases, which are important predictive factors associated with TNM staging.

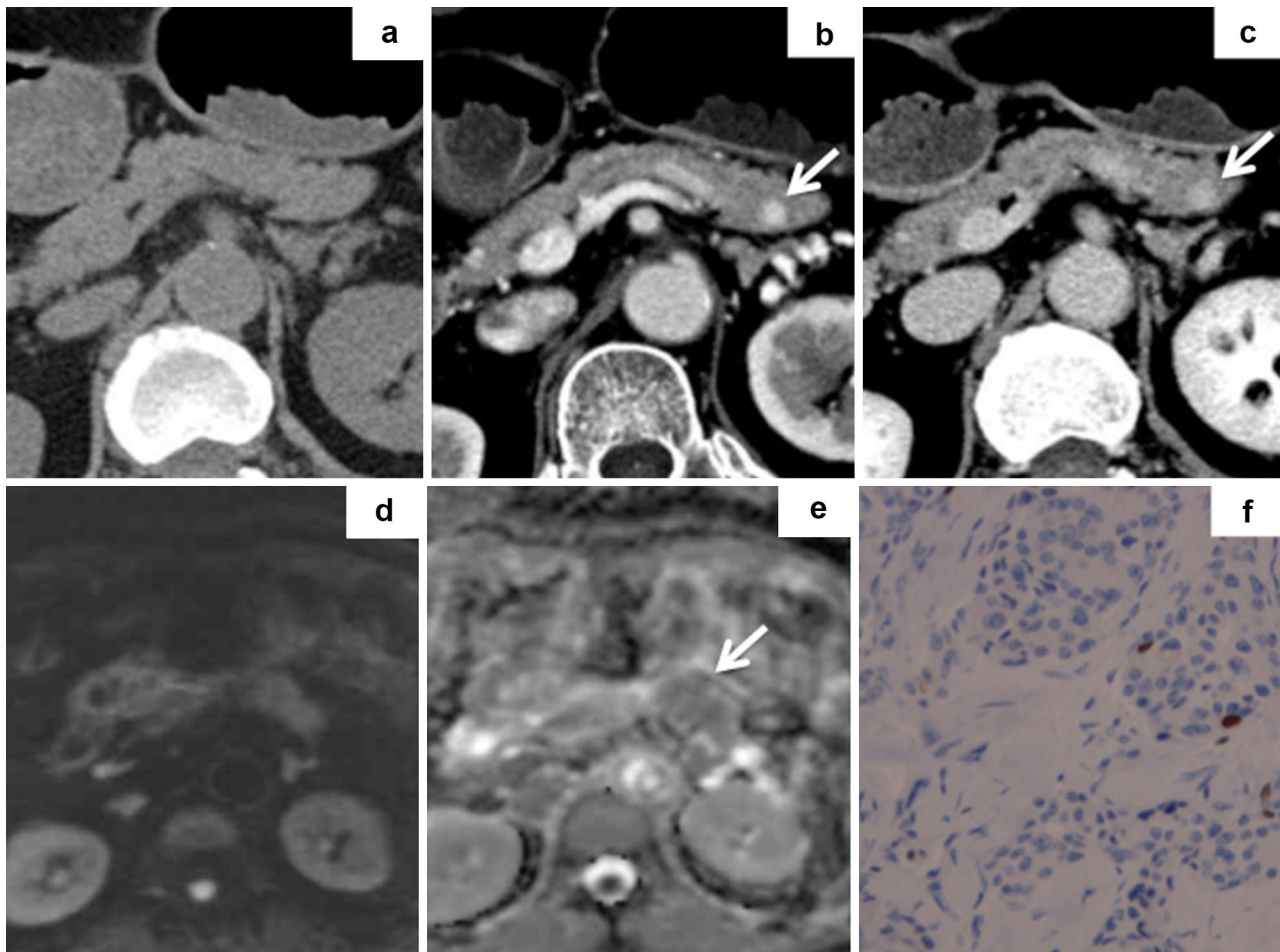


Fig. 2 G1 lesion in 78-year-old woman. **a** On plain CT image, the lesion cannot be discerned. **b** AP image on dynamic multiphase CT shows a small (9 mm), round, and homogeneous hyper-attenuating nodule in the pancreas body (*arrow*). **c** On delayed phase (DP) CT image, the lesion is seen as a slightly hyper-dense nodule (*arrow*) compared with pancreatic parenchyma. **d** On diffusion-weighted

(DW) MR image ($b = 800$), the lesion cannot be identified. **e** On ADC map ($b = 0\text{--}800$), the lesion (*arrow*) does not show reduction, compared with pancreatic parenchyma. ADC ratio is 1.06. **f** On immunohistochemistry of Ki-67, Ki-67 (*red-orange color*) index is less than 1%

Recently, the number of reports showing the utility of MR images [15–19], in particular ADC value, in tumor grading has been increasing. These studies have noted the mean ADC value of G1 lesions or well-differentiated neuroendocrine neoplasms to be $1.48\text{--}1.75 \times 10^{-3} \text{ mm}^2/\text{s}$, and that of G2, G3 lesions or neuroendocrine carcinoma $1.00\text{--}1.24$ [16–18]. Although the mean ADC value of each group in this study was not analyzed, because of the inconsistency of MR scanner and parameters due to the multi-institutional nature of the study, the result of ADC ratio (ADC value of the lesion/ADC value of the pancreatic parenchyma) and simple visual assessment for the ADC map (whether there was a reduction or no reduction, compared with the surrounding pancreatic parenchyma) were almost compatible with former studies. A recent study of intravoxel incoherent motion DW images also showed similar corresponding results [19].

In this study, PPV and NPV in the prediction of G1 for each single CT finding correlating with tumor grade (size, shape, and enhancement pattern on AP image) ranged from 70.5 to 86.3%, and 66.7 to 77.8%, respectively. These figures showed slight improvement by applying the combination pertaining to CT images. That is, small ($\leq 25 \text{ mm}$), round, and homogeneous early enhanced lesions, which are often suspected in routine practice of being typical PNETs [20], belonged to the G1 group with a probability of 89.1% (41 of 46 lesions). Conversely, the lesions with the opposite imaging findings (large size, lobulated shape, and no early enhancement pattern) belonged to G2 or G3 groups with a probability of 87.5%. Moreover, by assessing the MR finding (ADC) and CT image in combination, the predictive accuracy showed further improvement. That is, although the number of lesions was small (5 lesions), all of the lesions with the combination findings of low ADC ratio

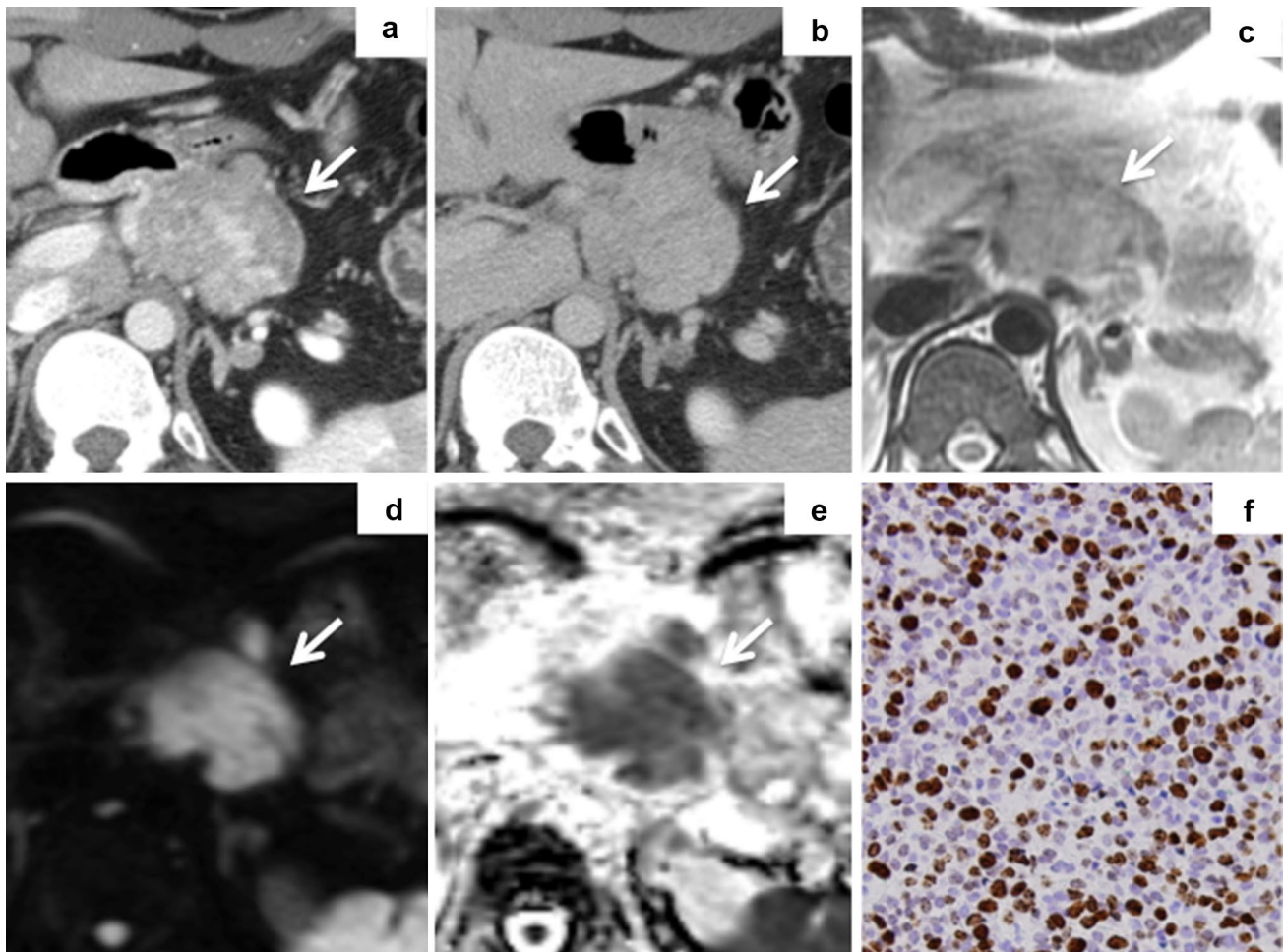


Fig. 3 G3 lesion in 28-year-old man. **a** AP image on dynamic multiphase CT shows a large (50 mm) heterogeneous attenuating lobulated mass (*arrow*). **b** On DP CT image, the lesion is seen as an iso- or slightly hyper-dense mass (*arrow*) compared with pancreatic parenchyma. **c** On T2-weighted MR image, the lesion dem-

onstrates heterogeneous slight hyper-intensity (*arrow*). **d** On DW image ($b = 800$), the lesion (*arrow*) is hyper-intense. **e** On ADC map ($b = 0\text{--}800$), the lesion (*arrow*) shows reduction. ADC ratio is 0.66. **f** On immunohistochemistry of Ki-67, Ki-67 (red-orange color) index is approximately 30%

($0.94 >$), no early enhancement pattern, lobulated shape, and hyper-intensity on T2-weighted image, belonged to G2 or G3 groups, and of these, 3 lesions were G3. In addition, all of the lesions (20 of 20 lesions) with high ADC ratio and small size (≤ 25 mm) were G1.

Based on the result of the combinational assessment, it was also revealed that in small tumors (≤ 25 mm), G2 or G3 lesions were present. Even in small tumors, the lesions not showing early homogeneous enhancement, and being reduced in ADC were considered to have the possibility of belonging to G2 or G3 group (66.7%).

We also performed multivariate analysis to find the independent factors in the imaging findings, which showed significant differences to univariate analysis. Multinomial logistic regression analysis in both CT and MR findings of 56 lesions showed that appearance on ADC map was only significantly associated with the tumor grade.

In recent routine clinical practice, with improvements in imaging techniques, and increase in the frequency of CT examination, the incidental detection of PNETs, small and non-functional lesions in particular, has increased. It was considered useful for patients with incidentally detected PNETs on CT images to also undergo MR examinations, because the results of multivariate and combinational analysis showed that the ADC finding was the important factor.

In routine clinical practice, distinguishing G3 lesions with the poorest prognosis from G1 or G2 lesions would be the most important task. G3 lesions tend to be large, lobulated, hypo-attenuating, and show a reduction in ADC (or lower ADC ratio) than G1 or G2 lesions. In addition, 3 of 5 lesions with the imaging findings of reduction in ADC, not homogeneous hyper-attenuation on AP CT image, lobulated shape, and hyper-intensity on T2-weighted image, belonged to G3, and even in small tumors, 2 of 12 lesions

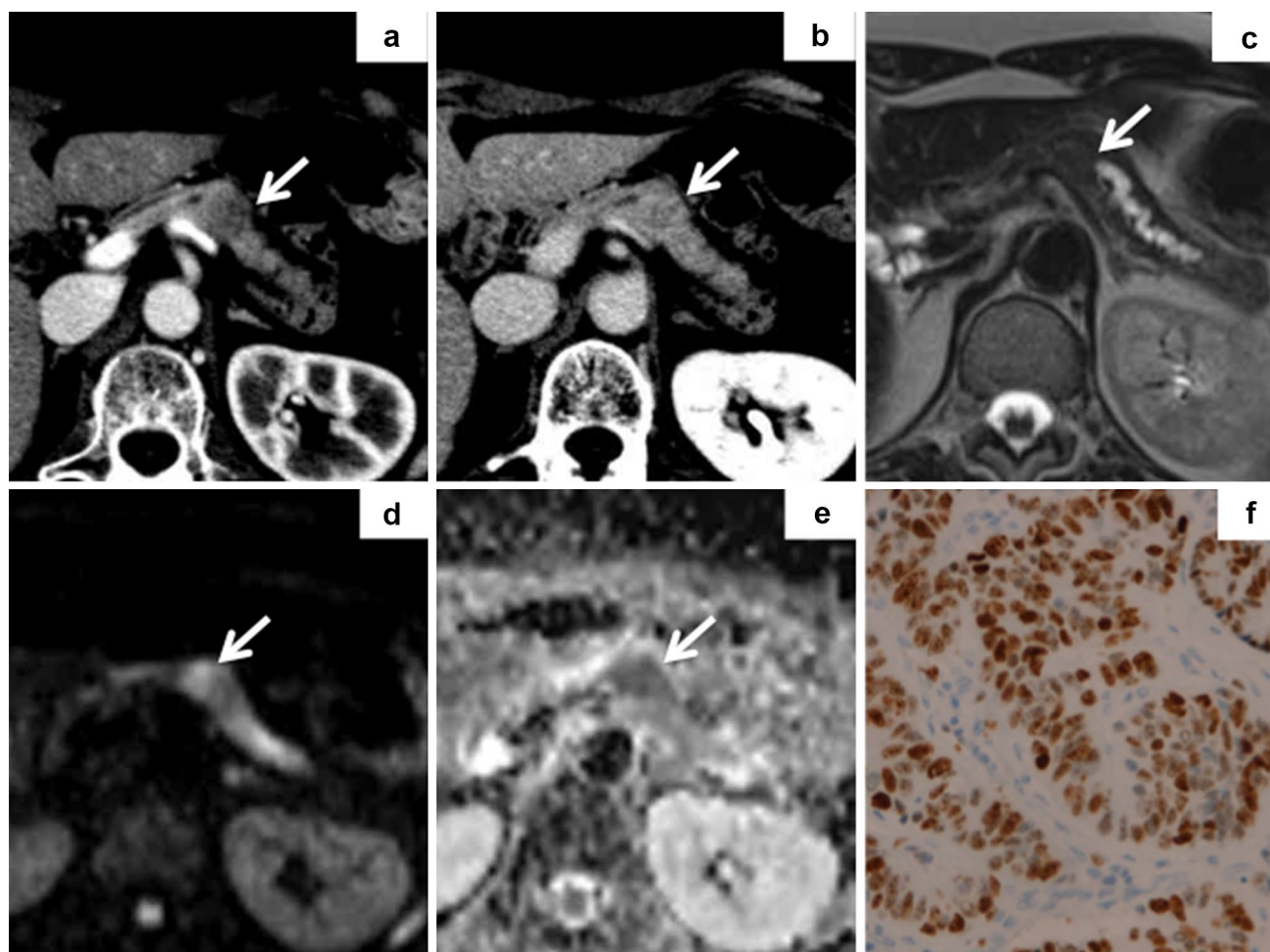


Fig. 4 G3 lesion in 62-year-old woman. **a** AP image on dynamic multiphase CT shows a small (17 mm) homogeneous hypo-attenuating nodule (*arrow*) in pancreas body. **b** On DP CT image, the lesion is seen as an iso- or slightly hyper-dense nodule (*arrow*) compared with pancreatic parenchyma. **c** T2-weighted MR image shows iso-

intense nodule (*arrow*) with distal main pancreatic duct (MPD) dilatation. **d** On DW image ($b = 800$), the lesion (*arrow*) is hyper-intense. **e** On ADC map ($b = 0\text{--}800$), ADC of the lesion (*arrow*) is reduced. ADC ratio is 0.55. **f** On immunohistochemistry of Ki-67, Ki-67 (red-orange color) index is approximately 80%

with the combination findings of reduction in ADC, and no early enhancement pattern were G3. However, no significant differences in any of these parameters, except lesion shape, were found in this study. This may be attributable to the small number of G3 lesions available for this study, because Kim et al. reported significant differences between G3 and G1/G2 lesions by analyzing the dynamic CT findings [14]. Just as combined assessment of CT and MR findings improved the predictive accuracy for G1 lesions in this study, useful findings predictive of G3 lesions might be found by multi-modality analysis with a large number of G3 lesions.

As with other pancreatic tumors, EUS-FNA plays an important role in diagnosing and grading of PNETs [21–25]. But it is a somewhat invasive and operator dependent procedure, and some complications including hemorrhage and pancreatitis have also been recognized. Also,

it is sometimes difficult to obtain sufficient tissue to adequately diagnose and grade the tumor [23–25]. A collaborative approach with imaging examinations and EUS-FNA would be essential for the optimal management of PNET patients.

Whether all PNETs should be resected immediately or not is a very important issue. At this time, all PNETs are considered as having malignant potential and surgical resection is recommended [26–28], but with the recent increasingly frequent detection of PNETs, the feasibility of careful follow-up especially of small PNETs, has been suggested [9, 27–29]. Observation should be considered in patients with small lesions, having the imaging findings for predicting G1 such as no reduction in ADC. However, for lesions with the imaging findings for suggesting G2 or G3 such as reduction in ADC and/or not homogeneous hyper-attenuation on AP CT image, the therapeutic approach

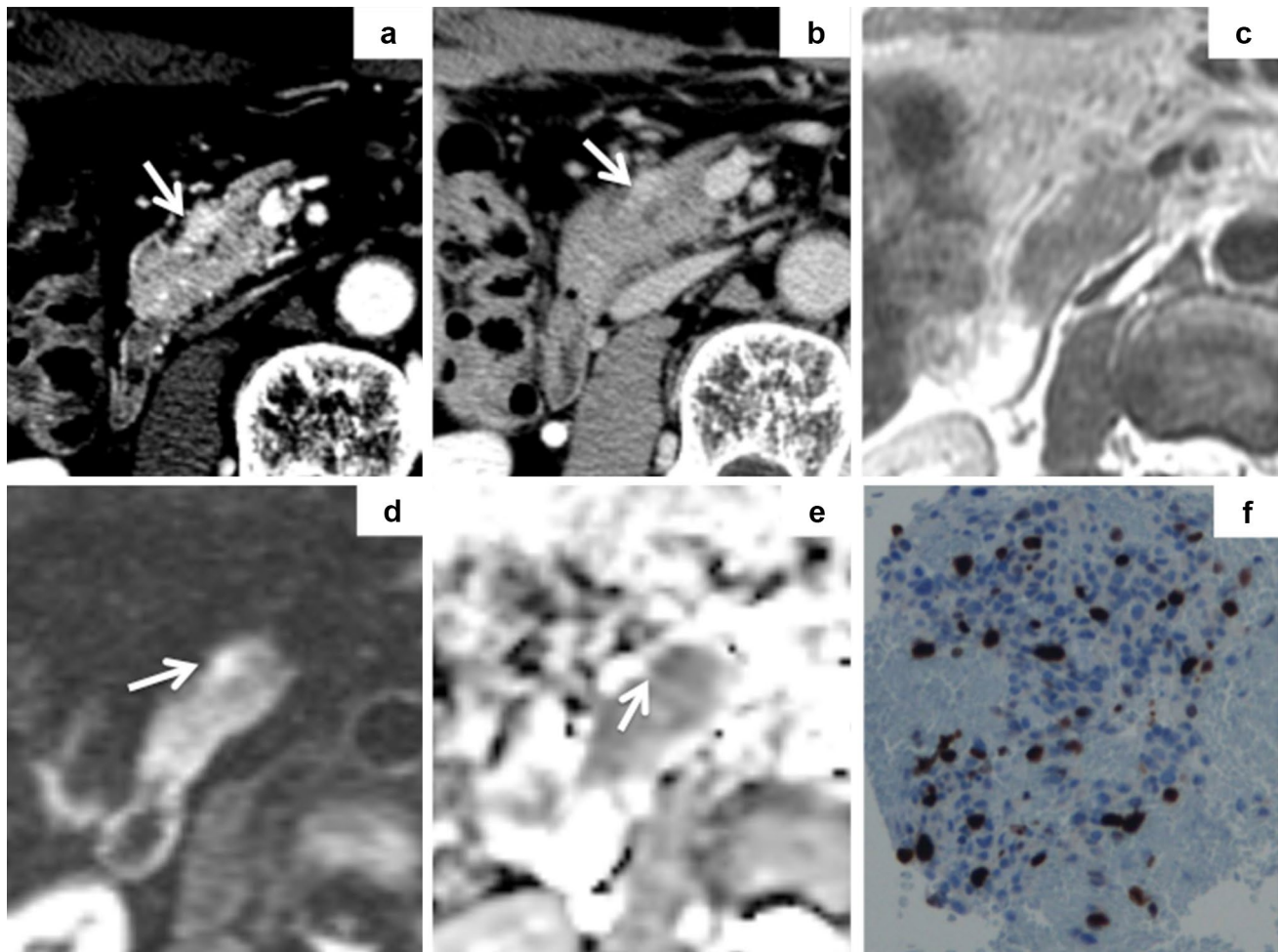


Fig. 5 G2 lesion in 72-year-old man (an endoscopic ultrasonography-guided fine needle aspiration case). **a** AP image on dynamic multiphase CT shows a small (10 mm) homogeneous hyper-attenuating nodule (*arrow*) in pancreas head. **b** On DP CT image, the lesion is seen as a slightly hyper-dense nodule (*arrow*) compared with pancre-

atic parenchyma. **c** On T2-weighted MR image, the lesion cannot be identified. **d** On DW image ($b = 800$), the lesion (*arrow*) is hyper-intense. **e** On ADC map ($b = 0\text{--}800$), ADC of the lesion (*arrow*) is reduced. ADC ratio is 0.81. **f** On immunohistochemistry of Ki-67, Ki-67 (*red-orange color*) index is approximately 10%

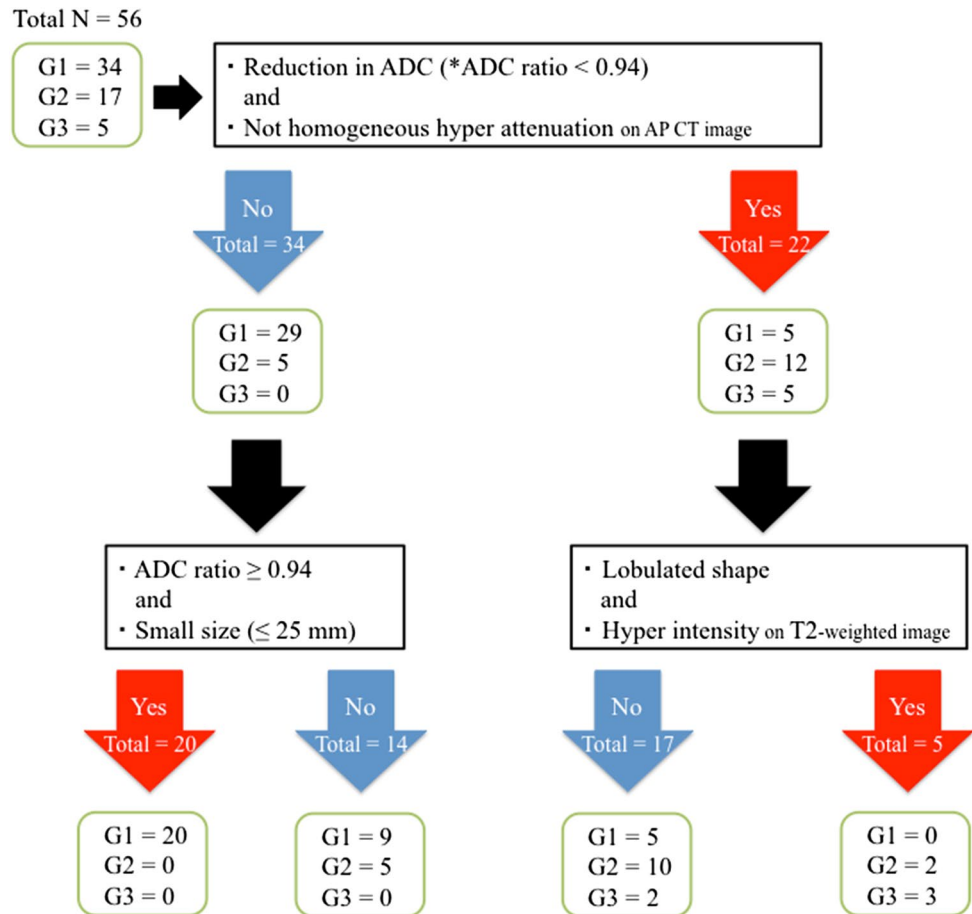
Table 2 Sensitivity, specificity, PPV and NPV in the prediction of G1 for each imaging finding

	Sensitivity	Specificity	PPV	NPV	Odds ratio (95% CL)
Diameter (≤ 25 mm)	86.4 (51/59)	59.5 (22/37)	77.3 (51/66)	73.3 (22/30)	9.35 (3.46–25.25)
Lesion shape (round)	93.2 (55/59)	37.8 (14/37)	70.5 (55/78)	77.8 (14/18)	8.37 (2.49–28.16)
Enhancement pattern on AP CT image	74.6 (44/59)	81.1 (30/37)	86.3 (44/51)	66.7 (30/45)	12.57 (4.58–34.53)
Absence of gradual enhancement	93.2 (55/59)	8.1 (3/37)	61.8 (55/89)	42.9 (3/7)	1.21 (0.26–5.76)
Absence of calcification	88.1 (52/59)	18.9 (7/37)	63.4 (52/82)	50.0 (7/14)	1.73 (0.55–5.42)
Absence of cystic portion	76.3 (45/59)	48.6 (18/37)	70.3 (45/64)	56.3 (18/32)	3.05 (1.26–7.35)
Absence of MPD dilatation	84.7 (50/59)	24.3 (9/37)	64.1 (46/78)	50.0 (9/18)	1.79 (0.64–5.02)
T1-weighted image (iso-intensity)	26.4 (14/53)	81.8 (27/33)	70.0 (14/20)	40.9 (27/66)	1.62 (0.55–4.73)
T2-weighted image (no hypo-intensity)	98.1 (52/53)	6.1 (2/33)	62.7 (51/83)	66.7 (2/3)	3.36 (0.29–38.56)
ADC map (no reduction in ADC)	70.6 (24/34)	81.8 (18/22)	85.7 (24/28)	64.3 (18/28)	10.80 (2.91–40.07)
ADC ratio ($0.94 \leq$)	70.6 (24/34)	92.3 (20/22)	92.3 (24/26)	66.7 (20/30)	24.00 (4.70–122.5)

Data are percentages, with number of lesions in parentheses

PPV positive predictive value, NPV negative predictive value, 95% CI 95% confidence intervals, AP arterial phase, MPD main pancreatic duct, ADC apparent diffusion coefficient

Fig. 6 A grading flowchart based on the combination of CT and MR findings. First, if the answers were ‘Yes’ to two questions pertaining to the MR and CT images, low ADC ratio (0.94>), and not homogeneous hyper-attenuation on AP image, 17 of 22 lesions belonged to G2 or G3 groups. Second, of 22 lesions (‘Yes’ group for first question), if the answers were ‘Yes’ to two questions, lobulated shape, and hyper-intensity on T2-weighted image, the rate of G2 or G3 was 100%. Third, of 34 lesions (‘No’ group for first question), if the answers were ‘Yes’ (high ADC ratio [0.94 or higher], and small size [25 mm or smaller]), the rate of G1 lesions was 100%. *ADC ratio ADC value of the lesion/ADC value of the surrounding pancreatic parenchyma



should be chosen carefully, because the possibility of malignancy exists even when they are small.

This study had a few limitations. First, because of its retrospective and multi-institutional nature, the CT and MR scanners, protocols, and contrast material were inconsistent. Second, our study included nine (10.1%) cases diagnosed and graded by EUS-FNA, although there was a potential for upgrade influenced by intra-tumor heterogeneity, when using a resected specimen [25]. Thus, we also analyzed in 87 resected lesions (the remaining 9 lesions diagnosed by EUS-FNA were excluded), and the results were similar to those of all lesions. Third, an ADC map was available for only 52 patients (58.4%). Lastly, our study included only a small number of G3 lesions, because of their lower frequency, namely only 6.8% of PNETs [7]. To more precisely define the most predictive imaging findings for G3 lesions, further study of a large number of G3 lesions might be required.

In conclusion, tumor size, shape, enhancement pattern including homogeneity on AP CT image, cystic degeneration, and ADC were correlated with the tumor grade of PNETs. Combined assessment of both MR and dynamic CT findings could improve the prediction of tumor grading in PNETs.

Funding The authors state that this work has not received any funding.

Conflict of interest The authors declare no conflict of interest associated with this manuscript.

References

1. Hruban RH, Pitman MB, Klimstra DS. Tumors of the pancreas. AFIP atlas of tumor pathology. 4th series fascicle 6. Washington: American Registry of Pathology; 2007.
2. Sahani DV, Bonaffini PA, Del Castillo CF, Blake MA. Gastroenteropancreatic neuroendocrine tumors: role of imaging in diagnosis and management. *Radiology*. 2013;266:38–61.
3. Klimstra DS, Arnold R, Capella, et al. Neuroendocrine neoplasms of the pancreas. In: Bosman F, Carneiro F, Hruban RH, Theise ND, editors. WHO classification of tumours of the digestive system. 4th ed. Lyon: IARC Press; 2010. p. 322–6.
4. Rindi G. The ENETS guidelines: the new TNM classification system. *Tumori*. 2010;96:806–9.
5. Rindi G, Klöppel G, Alhman H, et al. TNM staging of foregut (neuro) endocrine tumors: a consensus proposal including a grading system. *Virchows Arch*. 2006;449:395–401.
6. Rindi G, Klöppel G, Couvelard A, et al. TNM staging of midgut and hindgut (neuro) endocrine tumors: a consensus proposal including a grading system. *Virchows Arch*. 2007;451:757–62.

7. Rindi G, Falconi M, Klersy C, et al. TNM staging of neoplasms of the endocrine pancreas: results from a large international cohort study. *J Natl Cancer Inst.* 2012;10:764–77.
8. Ekeblad S, Skogseid B, Dunder K, Öberg K, Eriksson B. Prognostic factors and survival in 324 patients with pancreatic endocrine tumor treated at a single institution. *Clin Cancer Res.* 2008;14:7798–803.
9. Bettini R, Partelli S, Boninsegna L, et al. Tumor size correlates with malignancy in nonfunctioning pancreatic endocrine tumor. *Surgery.* 2011;150:75–82.
10. Takumi K, Fukukura Y, Higashi M, et al. Pancreatic neuroendocrine tumors: correlation between the contrast-enhanced computed tomography features and the pathological tumor grade. *Eur J Radiol.* 2015;84:1436–43.
11. d'Assignies G, Couvelard A, Bahrami S, et al. Pancreatic endocrine tumors: tumor blood flow assessed with perfusion CT reflects angiogenesis and correlates with prognostic factors. *Radiology.* 2009;250:407–16.
12. Rodallec M, Vilgrain V, Couvelard A, et al. Endocrine pancreatic tumours and helical CT: contrast enhancement is correlated with microvascular density, histoprognostic factors and survival. *Pancreatol.* 2006;6:77–85.
13. Luo Y, Dong Z, Chen J, et al. Pancreatic neuroendocrine tumours: correlation between MSCT features and pathological classification. *Eur Radiol.* 2014;24:2945–52.
14. Kim DW, Kim HJ, Kim KW, et al. Neuroendocrine neoplasms of the pancreas at dynamic enhanced CT: comparison between grade 3 neuroendocrine carcinoma and grade 1/2 neuroendocrine tumour. *Eur Radiol.* 2015;25:1375–83.
15. Manfredi R, Bonatti M, Mantovani W, et al. Non-hyperfunctional neuroendocrine tumours of the pancreas: MR imaging appearance and correlation with their biological behavior. *Eur Radiol.* 2013;23:3029–39.
16. Wang Y, Chen ZE, Yaghami V, et al. Diffusion-weighted MR imaging in pancreatic endocrine tumors correlated with histopathologic characteristics. *J Magn Reson Imaging.* 2011;33:1071–9.
17. Jang KM, Kim SH, Lee SJ, Choi D. The value of gadoxetic acid-enhanced and diffusion-weighted MRI for prediction of grading of pancreatic neuroendocrine tumors. *Acta Radiol.* 2014;55:140–8.
18. Kim JH, Eun HW, Kim YJ, Han JK, Choi BI. Staging accuracy of MR for pancreatic neuroendocrine tumor and imaging findings according to the tumor grade. *Abdom Imaging.* 2013;38:1106–14.
19. Hwang EJ, Lee JM, Yoon JH, et al. Intravoxel incoherent motion diffusion-weighted imaging of pancreatic neuroendocrine tumor: prediction of the histologic grade using pure diffusion coefficient and tumor size. *Invest Radiol.* 2014;49:392–402.
20. Lewis RB, Lattin GE Jr, Paal E. Pancreatic endocrine tumors: radiologic-clinicopathologic correlation. *RadioGraphics.* 2010;30:1445–64.
21. Rösch T, Lightdale CJ, Botet JF, et al. Localization of pancreatic endocrine tumors by endoscopic ultrasonography. *N Engl J Med.* 1992;326:1721–6.
22. Gouya H, Vignaux O, Augui J, et al. CT, endoscopic sonography, and a combined protocol for preoperative evaluation of pancreatic insulinomas. *AJR Am J Roentgenol.* 2003;181:987–92.
23. Ardengh JC, de Paulo GA, Ferrari AP. EUS-guided FNA in the diagnosis of pancreatic neuroendocrine tumors before surgery. *Gastrointest Endosc.* 2004;60:378–84.
24. Figueiredo FA, Giovannini M, Monges G, et al. EUS-FNA predicts 5-year survival in pancreatic endocrine tumors. *Gastrointest Endosc.* 2009;70:907–14.
25. Yang Z, Tang LH, Klimstra DS. Effect of tumor heterogeneity on the assessment of Ki67 labeling index in well-differentiated neuroendocrine tumors metastatic to the liver: implications for prognostic stratification. *Am J Surg Pathol.* 2011;35:853–60.
26. Hill JS, McPhee JT, McDade TP, et al. Pancreatic neuroendocrine tumors: the impact of surgical resection on survival. *Cancer.* 2009;115:741–51.
27. Falconi M, Bartsch DK, Eriksson B, et al. ENETS consensus guidelines for the management of patients with digestive neuroendocrine neoplasms of the digestive system: well-differentiated pancreatic non-functioning tumors. *Neuroendocrinology.* 2012;95:120–34.
28. National Comprehensive Cancer Network. NCCN clinical practice guidelines in oncology. Neuroendocrine tumors 2015 version 1. [National Comprehensive Cancer Network Web site]. <http://www.nccn.org/>. Accessed 30 Jan 2015.
29. La Rosa S, Klersy C, Uccella S, et al. Improved histologic and clinicopathologic criteria for prognostic evaluation of pancreatic endocrine tumors. *Hum Pathol.* 2009;40:30–40.